REPORT DOCUMENTATION PAGE			*Form Approved* *OMB No. 0704-0188*

The public reporting burden for this collection of information is estimated to average 1 hour per response, including the time for reviewing instructions, searching existing data sources, gathering and maintaining the data needed, and completing and reviewing the collection of information. Send comments regarding this burden estimate or any other aspect of this collection of information, including suggestions for reducing the burden, to Department of Defense, Washington Headquarters Services, Directorate for Information Operations and Reports (0704-0188), 1215 Jefferson Davis Highway, Suite 1204, Arlington, VA 22202-4302. Respondents should be aware that notwithstanding any other provision of law, no person shall be subject to any penalty for failing to comply with a collection of information if it does not display a currently valid OMB control number.
PLEASE DO NOT RETURN YOUR FORM TO THE ABOVE ADDRESS.

1. REPORT DATE *(DD-MM-YYYY)*	2. REPORT TYPE	3. DATES COVERED *(From - To)*
03/04/2019	Final technical report	07/01/2015-06/30/2018

4. TITLE AND SUBTITLE
DNA-based Nanofabrication of Functional Nanoscale Devices

5a. CONTRACT NUMBER N00014-15-1-2520
5b. GRANT NUMBER n/a
5c. PROGRAM ELEMENT NUMBER n/a

6. AUTHOR(S)
Liu, Haitao

5d. PROJECT NUMBER n/a
5e. TASK NUMBER n/a
5f. WORK UNIT NUMBER n/a

7. PERFORMING ORGANIZATION NAME(S) AND ADDRESS(ES)
UNIVERSITY OF PITTSBURGH
3520 FIFTH AVE
PITTSBURGH PA 15213-3320
UNITED STATES OF AMERICA

8. PERFORMING ORGANIZATION REPORT NUMBER
n/a

9. SPONSORING/MONITORING AGENCY NAME(S) AND ADDRESS(ES)
Office of Naval Research
875 N. Randolph Street Suite 1425
Arlington VA 22203-1995

10. SPONSOR/MONITOR'S ACRONYM(S)
ONR

11. SPONSOR/MONITOR'S REPORT NUMBER(S)
n/a

12. DISTRIBUTION/AVAILABILITY STATEMENT
approved for public release, distribution is unlimited

13. SUPPLEMENTARY NOTES
n/a

14. ABSTRACT
The objective of this project is to develop a toolkit to enable DNA-based multi-step nanofabrication of functional semiconductor nano-electronic devices. The research will address two major challenges that are central to the DNA-based nano-manufacturing in semiconductor industry: (1) programmable, self-aligned deposition of DNA templates for multi-step nanofabrication; and (2) site-specific doping of Si and other inorganic semiconductor substrate using a DNA template. If successful, this project will demonstrate the fabrication of Si transistors using DNA lithography as the patterning tool.

15. SUBJECT TERMS
n/a

16. SECURITY CLASSIFICATION OF:			17. LIMITATION OF ABSTRACT	18. NUMBER OF PAGES	19a. NAME OF RESPONSIBLE PERSON
a. REPORT	b. ABSTRACT	c. THIS PAGE			Haitao Liu
			SAR		19b. TELEPHONE NUMBER *(Include area code)* (412)624-2062

Standard Form 298 (Rev. 8/98)
Prescribed by ANSI Std. Z39.18

Final Technical Report

Award Title: **DNA-Based Nanofabrication of Functional Nanoscale Devices**

ONR Award Number: **N00014-15-1-2520**

Reporting period: **July 1st 2015 to June 30th, 2018**

Principal Investigator Name: **Professor Haitao Liu**

Organization: **University of Pittsburgh**

Distribution Statement

DISTRIBUTION A. Approved for public release: distribution unlimited.

Research Accomplishments

During the funding period, we have made significant progress in the DNA-based patterning of substrate, including but not limited to the patterning of dopant atoms in a site-specific manner. We encountered many difficulties in developing aligned deposition of DNA nanostructures. The most significant accomplishments are:

1.Developed a DNA-based patterning of self-assembled monolayers. This result paves the way to use DNA to deliver dopant to Si wafers with nanoscale resolution and specificity.

2. Developed a DNA-based imprinting lithography method to pattern polymer substrate. This technology could pave the way to dope organic/polymer semiconductors using DNA.

Detailed Accomplishments

1. DNA-based patterning of self-assembled monolayers.

Introduction. Forming self-assembled monolayer (SAM) is a widely used approach to control and modify the surface properties, such as wetting, adhesion, surface potential, and surface chemistry. In particular, it has been shown that SAMs containing phosphorous and boron atoms can dope Si wafer when heated at high temperature.[1-2] For this reason, we are interested in developing a DNA based patterning of SAM structures. A variety of methods have been developed to pattern SAMs. Top down approaches such as photoliothography, e-beam lithography, dip-pen nanolithography, and soft lithography have been used to pattern single- and multi-component SAMs.[3-8] Various bottom-up approaches have also been reported in the literature, where a mixture of silanes was allowed to adsorb simultaneously or sequentially on the substrate.[9-13] Scanning probe microscopy or a combination of scanning probe microscopy and self-assembly has been developed to obtain mixed SAMs with well-ordered domains. In one approach, a tip is used to mechanically remove part of the SAM from the substrate surface followed by backfilling with another SAM precursor; alternatively, the tip applies an electrical bias to oxidize or reduce the mixed self-assembled monolayers resulting in mixed SAM.[14-17] In another method known as magnetolithography, a surface is patterned using superparamagnetic nanoparticles that are assembled by magnetic field.[18-19] This method provides high resolution patterning at large length scales for even non-flat and tubular shaped substrates.

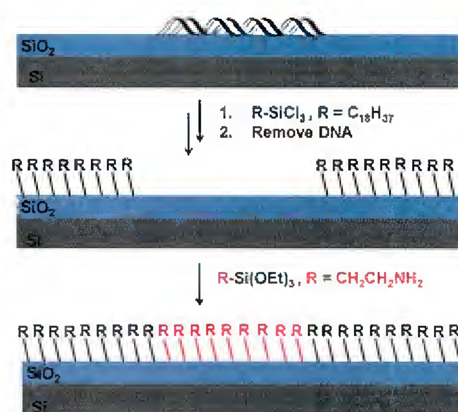

Figure 1.1. Patterning mixed silane SAMs using a DNA template. DNA nanostructures are deposited on a substrate and exposed to octadecyltrichlorosilane vapor followed by removal of DNA, resulting in negative tone patterns in the octadecyltrichlorosilane SAM. The patterned SAM is then exposed to 3-aminopropyl triethoxy silane (APTES) vapor, resulting in a patterned mixed SAMs.

Despite these advances, none of the current method offers a solution to low cost, high throughput patterning of SAM with arbitrary-shaped patterns at the sub-10 nm length scale. For example, while approaches based on phase separation and self-assembly have the cost and throughput advantage, it is difficult to form arbitrary-shaped patterns. Approaches based on top-down lithography suffer from either limited resolution (e.g., photolithography and soft lithography) or requiring dedicated, expensive instruments (e.g., e-beam lithography and dip-pen lithography).

Using DNA nanostructure as a mask to pattern SAM could potentially offer the best of both top-down and bottom-up approaches: scalability, low cost, high resolution, and capability to produce arbitrary shape. There was no previous report on using unmodified DNA nanostructures as mask to block surface reactions. Although DNA nanostructures have been used to pattern vapor phase metal deposition,[20-21] the much faster diffusion of small organic reagents poses significant challenges, especially considering the molecular thinness and absence of covalent crosslinking in unmodified DNA structures. Herein we report the first use of DNA nanostructures as a masking template to pattern SAM. We show that DNA nanostructures can block the diffusion of reagents to react with the substrate, resulting in a faithful pattern transfer to the SAM.

Results and discussion. Figure 1.1 outlines the strategy we took to pattern silane SAM with DNA templates. Our approach relies on the vapor phase deposition of silane precursor onto a Si substrate that has a thin layer of native SiO_2 (Si/SiO_2 substrate). Briefly, DNA nanostructures were assembled on the Si/SiO_2 substrate and placed inside a glass container. The pressure inside the container was reduced to vaporize octadecyltrichlorosilane (ODTCS). The ODTCS vapor deposited on and around the DNA on the Si/SiO_2 substrate. On sonication in deionized water, the DNA nanostructures fell off the substrate resulting in negative tone patterns of ODTCS monolayers on the Si/SiO_2 substrate. The patterned SAM can be backfilled with a different silane to produce a mixed SAM (see below).

Figure 1.2a shows the AFM image and the cross section of triangular DNA nanostructures assembled on the Si/SiO_2 substrate. After exposing the Si/SiO_2 substrate containing DNA nanostructures to ODTCS vapor, the apparent height of the DNA nanostructure increased from ca. 1.5 nm to ca. 4.0 nm, suggesting that the silane deposited on the SiO_2 surface as well as on the DNA nanostructures (**Figure 1.2b**). After a brief sonication in deionized water, the DNA nanostructures readily fell off resulting in negative tone triangular patterns that are ca. 2 nm deep. The depth of the trenches is similar to that of the thickness of ODTCS SAM, suggesting that the bottom of the trenches is likely exposed SiO_2 surface (**Figure 1.2c**).

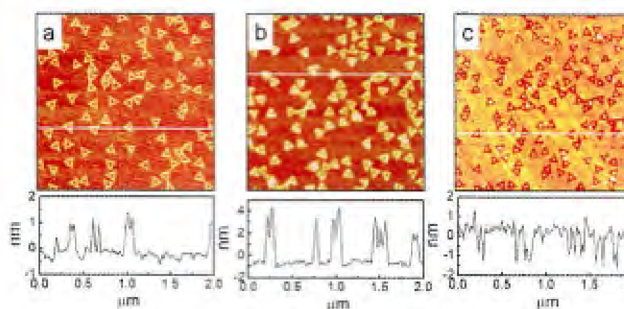

Figure 1.2. AFM images and cross sections of (a) DNA nanostructures assembled on a Si substrate. (b) Sample (a) after exposure to ODTCS. (c) Sample (b) after sonication in DI water to remove DNA. The white line indicates the line of cross section.

The above observations suggest that the DNA nanostructures are capable of blocking the diffusion and/or reaction of ODTCS molecules to the underlying SiO_2 surface. It is commonly accepted that the DNA nanostructures are anchored to the SiO_2 surface through electrostatic interaction mediated by Mg^{2+}. In contrast, ODTCS is capable of forming covalent bond with the SiO_2 surface. Given these considerations, it is not entirely surprising that the DNA nanostructures can be easily removed by sonication without damaging the ODTCS SAM.

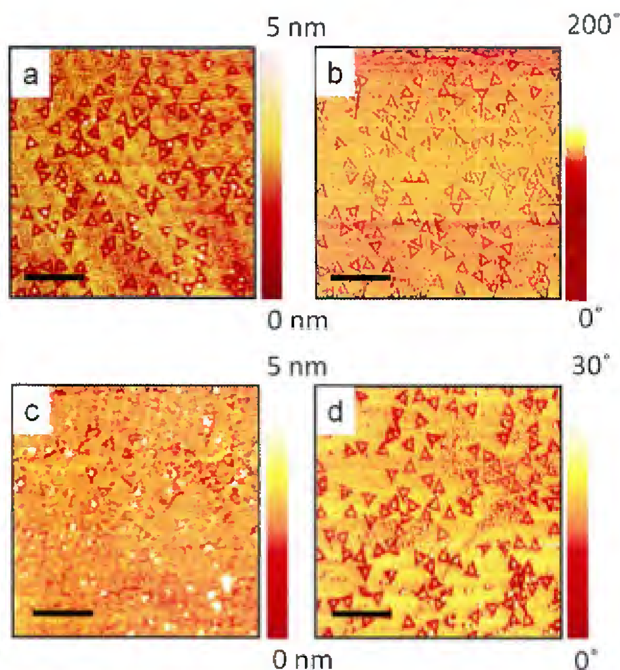

Figure 1.3. Fabrication of mixed monolayer SAM. (a) and (b) are the AFM topography and phase images of ODTCS pattern on the Si substrate. (c) and (d) are the AFM topography and phase images of bilayer silane pattern of APTES and ODTCS. APTES is deposited on the ODTCS pattern substrate at vapor phase resulting in bilayer silane pattern. Scale bar: 500 nm.

To form a mixed SAMs, a negative tone patterned ODTCS SAM was prepared and then exposed to 3-aminopropyltriethoxysilane (APTES) vapor. The APTES molecules selectively deposited onto the trenches where the SiO_2 was exposed, resulting in the formation of mixed SAMs patterns with nanoscale resolution. To verify the formation of mixed SAM, we analyzed the change in the AFM topography and phase images after the backfilling. We note that the AFM phase contrast is generated due to the difference in the energy dissipation involved in the contact between the AFM tip and the sample; the energy dissipation depends on the properties of the surface, such as visocoelasticity and adhesion; the phase will therefore depend on the chemical nature of the sample surface.[22-23] As a result, two surfaces having similar topography but different chemical composition can be easily identified in AFM phase imaging.

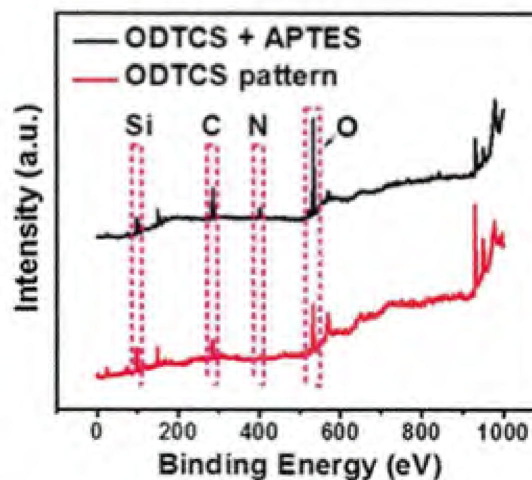

Figure 1.4. XPS survey scan of patterned ODTCS SAM (red) and mixed ODTCS/APTES SAM on silicon substrates.

Figure 1.3a and 3b show the AFM topography and phase images of the negative-tone ODTCS patterns formed on a Si/SiO_2 substrate, respectively. Both the images show distinct triangular patterns consistent with the negative-tone ODTCS pattern

after the removal of DNA template. After exposing the ODTCS patterned substrate to an APTES vapor, we observed a significant decrease in the topography contrast. As shown in **Figure 1.3c**, the trenches are barely visible in the topography image, consistent with the back filling of the trenches with APTES. In contrast, in the phase image shown in **Figure 1.3d**, the triangular patterns are still clearly visible, consistent with the back-filling of APTES. In addition to the AFM characterization, the XPS spectrum (**Figure 1.4**) of the patterned ODTCS sample showed presence of Si, O, and C peaks, while that of APTES-backfilled sample showed an additional N peak due to the incorporation of APTES. These results strongly support the formation of mixed monolayer SAM in our experiments.

Conclusion. In conclusion, we have demonstrated a novel approach to pattern single-component and mixed SAMs with nanometer scale resolution using DNA nanostructure as a template. Our result shows that even a single layer of close-packed double-stranded DNA is capable of blocking the diffusion of SAM precursor to the underlying SiO_2 substrate. This technique opens up new opportunities to use DNA nanostructure as a blocking template for nanofabrication. In the present study, the DNA nanostructure templates are randomly deposited onto the substrate. For many applications (*e.g.*, nanolithography), it is desirable to have control over the position and orientation of the DNA templates. Ways to deterministically position DNA nanostructures onto a substrate have been reported;[15] work to integrate these approaches with DNA-mediated patterning of SAMs will be explored in the future.

2. DNA nanostructure for high resolution imprinting lithography

Introduction. Soft lithography uses a stamp to transfer micro- and nano-scale patterns.[24-28] The stamp is usually fabricated by casting a liquid precursor onto a master template with patterned structures. Soft lithography has been well developed and widely used for nanofabrication due to its simplicity, low cost, and compatibility with a wide range of substrates, especially soft materials and nonplanar surfaces.[25, 28-29] The application of soft lithography, however, is fundamentally limited by the spatial resolution and diversity of the structures on the stamp.

Significant efforts have been put into the preparation of master templates, from which the stamp is derived.[28, 30] Conventional lithography methods, such as photolithography and electron-beam (e-beam) lithography, are the most general approach to fabricating master templates. One-step 193-nm photolithography is widely used; however, it is not suitable for the fabrication of nanostructures with spacing less than 40 nm due to its diffraction-limited resolution. Although e-beam lithography can provide sub-10-nm resolution, the massive production of the master template is hindered by the high cost of this method.[31-33] In addition to the conventional lithographic methods, dip-pen nanolithography,[34] indentation lithography,[35] nanosphere lithography,[36] and block copolymer lithography[37-40] have been applied to offer nanoscale and even sub-10-nm features. Other relief structures such as crystallographic steps,[41] cracks,[42] and single-walled carbon nanotubes[43] have also been used to provide features with sub-nanometer or molecular-scale resolution. However, it still remains a challenge to develop a general method of

constructing master templates and stamps with diverse nanoscale features and high spatial resolution.

In recent years, programmable DNA self-assembly[44-46] has produced a wide range of one-dimensional (1D),[47-50] two-dimensional (2D)[51-56] and three-dimensional (3D)[57-62] nanostructures with diverse and complex features. Assembled DNA nanostructures can be rationally designed and reliably synthesized. The assembly process is fast and easily implemented.[63] Thus, self-assembled DNA nanostructures can be used as a nanofabrication template due to ease of controlling their shapes with nanometer-scale spatial resolution. Along this direction, many approaches have been developed to transfer the pattern of DNA nanostructures to a wide range of materials. We briefly review these efforts below.

DNA nanostructures have been employed as masks to transfer the pattern to evaporated noble metal films.[21] Metallization has also been achieved through wet chemistry, and the resulting metal nanostructures have been used to pattern graphene.[64] By exploiting the difference in adsorption of water between DNA nanostructures and a SiO_2 substrate, DNA nanostructures have been used to modulate the rate of HF vapor phase etching to achieve pattern transfer to the SiO_2 substrate.[65] Based on the same principle, adsorption of water could control the rate of chemical vapor deposition of SiO_2 and TiO_2 on the DNA nanostructures and substrate to convert the pattern of DNA nanostructures into that of inorganic oxides.[66] Moreover, Al_2O_3 protected DNA nanostructures can be converted to carbon nanostructures by thermal annealing.[67] In addition to the 2D pattern transfer, DNA 3D nanostructures have served as molds to synthesize inorganic nanostructures with prescribed 3D shapes.[68]

DNA nanostructures are promising templates for materials science due to their structural complexity and diversity in the nanoscale. However, nanofabrication based on DNA nanostructures still faces several formidable challenges. First of all, the high cost of synthetic DNA hinders its application as a master template for large scale patterning.[69] Second, there is a lack of reliable and faithful pattern transfer method that is compatible with existing fabrication processes due to the low mechanical and chemical stability of DNA nanostructures. Third, deterministic deposition of DNA nanostructures, which is critical to large-area fabrication, is still in its infancy. Existing approaches to controlling the deposition of DNA nanostructures suffer from low fidelity and high error rate.[70-73]

A strategy to partially overcome these problems is to establish a method to transfer complex DNA patterns to a polymer substrate. The resulting polymer stamps can be used as templates for the following patterning process, which reduces the cost, simplifies the fabrication process and potentially overcomes the difficulties of scalable patterning. Recently, a linear DNA bundle with an average height of *ca.* 90 nm and an average width of *ca.* 879 nm was employed as a master template for the fabrication of a negative replica on an unsaturated polyester resin which was further used to pattern a polyacrylamide gel.[74] However, the lateral dimension of the DNA bundle is relatively large (*ca.* 1 μm). To the best of our knowledge, none of the nanoscale DNA structures have been used as templates to fabricate polymer stamps with high diversity, complexity and fidelity.

Herein we demonstrate an approach to using DNA nanostructures as master templates in a direct pattern transfer from DNA to polymers with high fidelity. The nanoscale features of the polymer can be rationally controlled by the design of the DNA nanostructures. A variety of DNA nanostructures were used to pattern poly(methyl methacrylate) (PMMA) and poly(L-lactic acid) (PLLA), including DNA nanotubes, 1D λ-DNA, 2D DNA brick crystals with 3D features, hexagonal DNA 2D arrays, and triangular DNA origami. The resulting polymer stamp could serve as a mold to transfer the pattern to an acryloxy perfluoropolyether (a-PFPE) polymer substrate.

Results and Discussion. The fabrication of polymer stamps consists of six steps as shown in **Figure 2.1**.[75] A silicon wafer with native oxide was cleaned by piranha solution and served as a substrate for DNA deposition (**Figure 2.1**, **a** to **b**). After the DNA nanostructure was deposited, a polymer film (*e.g.*, PMMA) was spin-coated on the substrate to cover the DNA (**Figure 2.1**, **b** to **c**). A negative replica formed on the sub-surface of the film which was in contact with the DNA. Four edges of the film were scratched to expose the underlying silicon substrate (**Figure 2.1**, **c** to **d**). Then a polydimethylsiloxane (PDMS) film was adhered to the polymer film as a flexible backing to assist in removing the polymer film from the silicon substrate in the next step (**Figure 2.1**, **d** to **e**). Drops of water were added to one edge of the exposed silicon substrate and were allowed to penetrate into the interface between the hydrophobic polymer and the hydrophilic silicon wafer. In the last step, the PDMS/polymer film was peeled off and gently dried by a nitrogen stream (**Figure 2.1**, **e** to **f**). The whole process can be completed in several minutes.

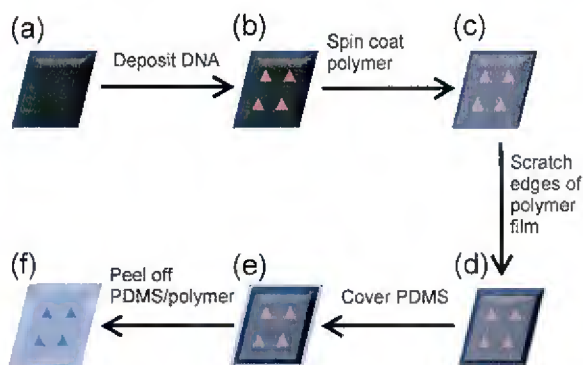

Figure 2.1. Fabrication of polymer stamps using DNA nanostructures as master templates. (a) The silicon wafer. (b) DNA is deposited on the silicon wafer. (c) A polymer film (*e.g.*, PMMA) is spin-coated on the silicon wafer. (d) Polymer film (*ca.* 1 mm wide) is removed from the four edges. (e) A polydimethylsiloxane (PDMS) film adheres to the polymer film as a flexible backing. (f) Drops of water are added to one edge of the exposed silicon wafer and the PDMS/polymer film is peeled off.

We first demonstrate the stamp fabrication using self-assembled DNA nanotubes which have a length of up to 60 μm and a width in the range of 30–70 nm.[48] The topography of the DNA master templates and polymer stamps were characterized by atomic force microscopy (AFM). In the AFM images, the height of the DNA nanotubes was measured to be 4.0 ± 0.5 nm. This small

height is expected due to the collapse of the DNA nanotubes during the drying process (**Figures 2.2a**). Bundling of DNA nanotubes, however, was evident in some areas. After the polymer film was peeled off, the trenches corresponding to the DNA nanotubes was observed on the PMMA stamp. The 1D trenches were 3.2 ± 0.7 nm in depth, in good agreement with the height of the DNA nanotube master templates (**Figures 2.2b**). The measured width of the nanotube master template (67.1 ± 5.3 nm) was larger than the expected value, and the measured width of the 1D trenches on the PMMA stamps (39.7 ± 5.1 nm) was smaller than the expected value. We attribute this observation to the AFM probe convolution effect and the removal of the salt residues during the fabrication of the PMMA stamp. The bundling of DNA nanotubes produced wider and deeper 1D trenches. These results confirm a successful replication process from the DNA nanotubes to the PMMA stamp.

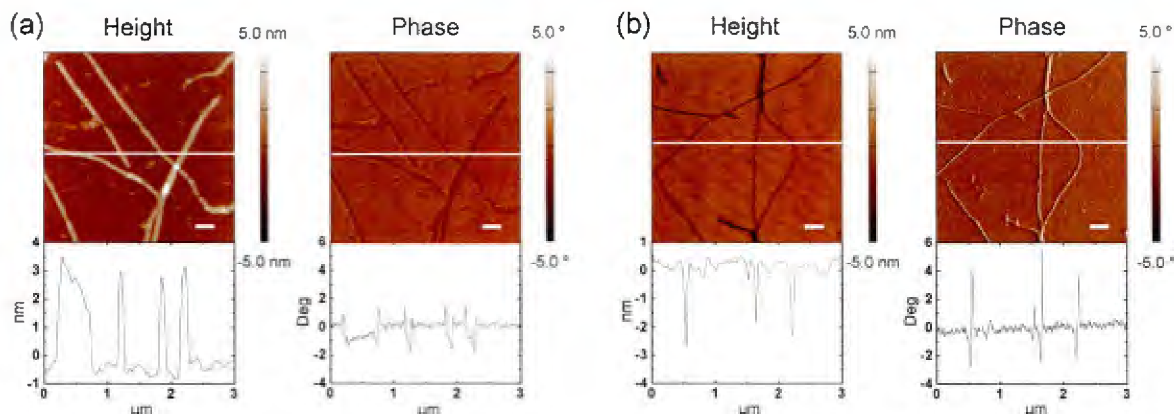

Figure 2.2. Fabrication of PMMA stamps by replication over DNA nanotubes. AFM height (left) and phase (right) images of (a) DNA nanotubes deposited on the silicon wafer and (b) the replica of nanotube patterns on PMMA stamps (top). Corresponding cross-sections are shown at the bottom. Scale bars represent 300 nm.

A similar stamp fabrication method was reported to replicate the pattern of single-walled carbon nanotubes (SWNTs) to high-modulus (~ 10 MPa) PDMS.[43] In that method, SWNTs attach to the silicon wafer through van der Waals interaction. In addition, an anti-adhesion silane layer has to be deposited on the wafer to reduce the adhesion of PDMS to the silicon wafer. In our method, however, DNA nanostructures and the silicon wafer are bound through Mg^{2+}, *via* a likely much stronger electrostatic interaction. In addition, water can easily separate the hydrophilic silicon wafer from the hydrophobic polymer stamp, and the anti-adhesion silane layer is not required. Most importantly, our method can produce diverse nanostructures instead of simple linear trenches (see below).

Besides 1D nanostructures, 2D DNA brick crystals with defined 3D features could also serve as master templates to transfer 3D patterns to PMMA. Such 2D DNA brick crystals were prepared through the recently developed "DNA bricks" approach.[76] After a one-pot annealing process, 2D DNA brick crystals with parallel channels were assembled (**Figure 2.3a**). The

channels are designed to be 10 nm high and 15 nm wide, and are separated by ridges with a height of 10 nm and a width of 15 nm (**Figure 2.3b**), assuming 2.5-nm diameter per hydrated DNA helix.[76] The assembled brick crystals were imaged by transmission electron microscopy (TEM). The parallel channels were clearly visible in the TEM image, and the measured pitch of the brick crystal was 24.9 ± 0.5 nm, smaller than the theoretical value of 30 nm (**Figure 2.3c**). The decreased pitch of the 2D brick crystals is attributed to the staining and dehydration of the DNA brick crystals during TEM sample preparation and imaging in vacuum. The AFM images show a consistent shape of the 2D brick crystals (**Figures 2.3d**). The height of the 2D brick crystals in the AFM image was 7.3 ± 0.3 nm, which is much smaller than the theoretical value of 20 nm, and the pitch was 29.9 ± 1.8 nm (expected value: 30 nm). The trenches within the DNA brick crystal were clearly visible in the AFM phase image; however, their full depth was not resolved in the topography image, likely due to the tip convolution effect. In addition, a high concentration of magnesium ions (40 mM) had to be used to stabilize the DNA brick crystals, resulting in the aggregation of DNA brick crystals (**Figures 2.3d - e**).

After the replication process, the negative replica of the DNA brick crystal could be clearly seen on the PMMA film (**Figures 2.3e**). The depth of the negative replica pattern was 7.7 ± 0.3 nm, in good agreement with that of the original 2D brick crystal (7.3 ± 0.3 nm) on the silicon wafer (**Figure 2.3e**). The trenches within the negative replica were clearly visible in the phase image and the pitch was 30.3 ± 0.6 nm, which is close to that of the DNA master template (**Figure 2.3e**). Although the trenches were clearly visible in the topography image, their depth was not fully resolved and is much smaller than the expected value of 10 nm. This observation is similar to that of the DNA brick crystals. Nevertheless, the consistency of the shape, height, and pitch between 2D DNA brick crystals and their replica on PMMA stamps indicates a faithful replication process.

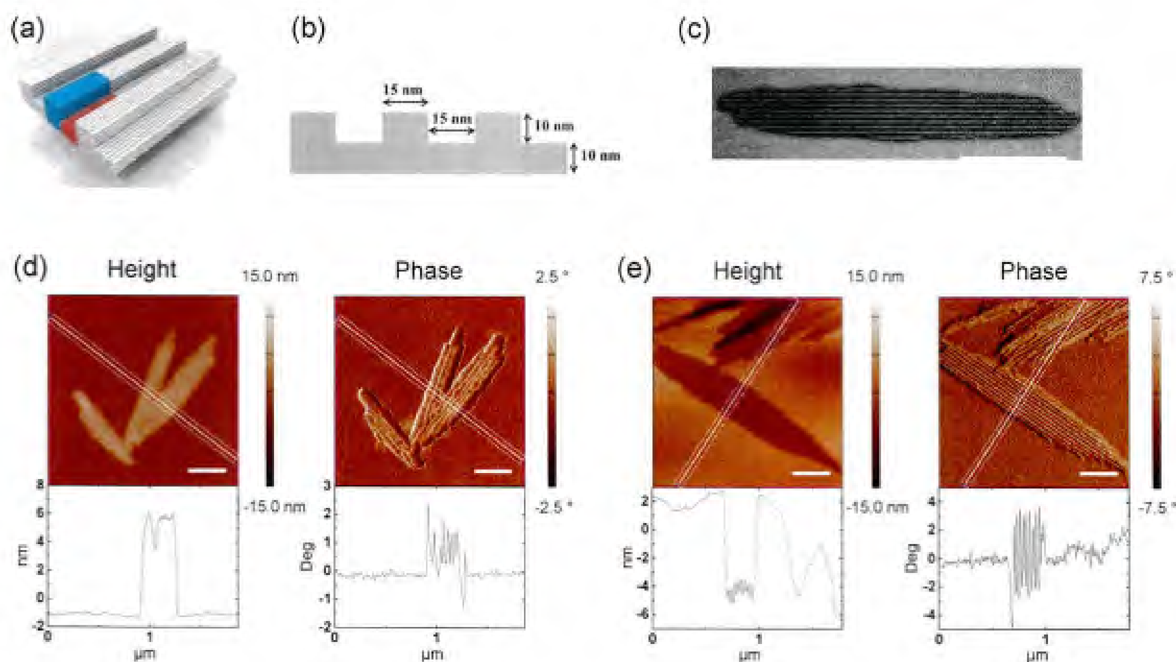

Figure 2.3. Fabrication of PMMA stamps by replication over 2D DNA brick crystals. (a) A model of 2D DNA brick crystal. The repeating unit is labeled as the blue and orange block. (b) Side view of the model of the 2D DNA brick crystal. (c) The transmission electron microscopy (TEM) image of the 2D DNA brick crystal. The scale bar represents 500 nm. (d) AFM height (left) and phase (right) images of 2D DNA brick crystals deposited on a silicon wafer (top) and the corresponding cross-sections (bottom). (e) AFM height (left) and phase (right) images of the replica of 2D DNA brick crystals on PMMA stamps (top) and the corresponding cross-sections (bottom). Scale bars in d and e represent 300 nm.

In addition to the DNA nanotubes and the 2D DNA brick crystals, DNA nanostructures with smaller feature sizes could also be used as master templates in our method. A hexagonal DNA 2D array was tested as a master template for the pattern transfer. The hexagonal DNA 2D array was self-assembled from DNA 3-point-star motifs (**Figure 2.4a**).[52] Each edge of the motif consists of two DNA double strands with a length of 4.5 turns. To increase the surface coverage of the DNA 2D arrays, silicon substrate mediated annealing was used to directly grow the DNA 2D arrays on the silicon wafer.[77-78] A freshly cleaned silicon wafer was immersed in the DNA solution and annealed with DNA strands from 95 °C to 23 °C in one day. During this process, DNA motifs were adsorbed and confined to the SiO_2 surface to facilitate the self-assembly.[50] **Figures 2.4b** shows that after the annealing, most areas of the silicon wafer were covered by a monolayer of DNA 2D arrays with a hexagonal shape. The Fourier transform of the AFM phase image shows the expected six-fold symmetry of the DNA array (**Figure 2.4c**). Big white spots were also observed, which we attribute to DNA aggregates and salt residues attached to the monolayer DNA. The section analysis shows that the repeating distance of the DNA 2D array was 29.7 ± 0.7 nm, in good agreement with the theoretical value of 30.3 nm.[52] On the surface of PMMA, the negative replica of the DNA 2D array appeared as an array of pillars and was highlighted by the white arrows in **Figures 2.4d**. The Fourier transform of the pattern shows six-fold symmetry which is consistent with the pattern of the DNA master template (**Figure 2.4e**). The periodicity of the pattern was measured by the averaged distance between adjacent pillars and found to be 29.7 ± 0.9 nm, almost identical to that of the DNA master template. The pillar-like PMMA pattern of the same symmetry and periodicity confirms the pattern replication from DNA 2D arrays to PMMA stamps.

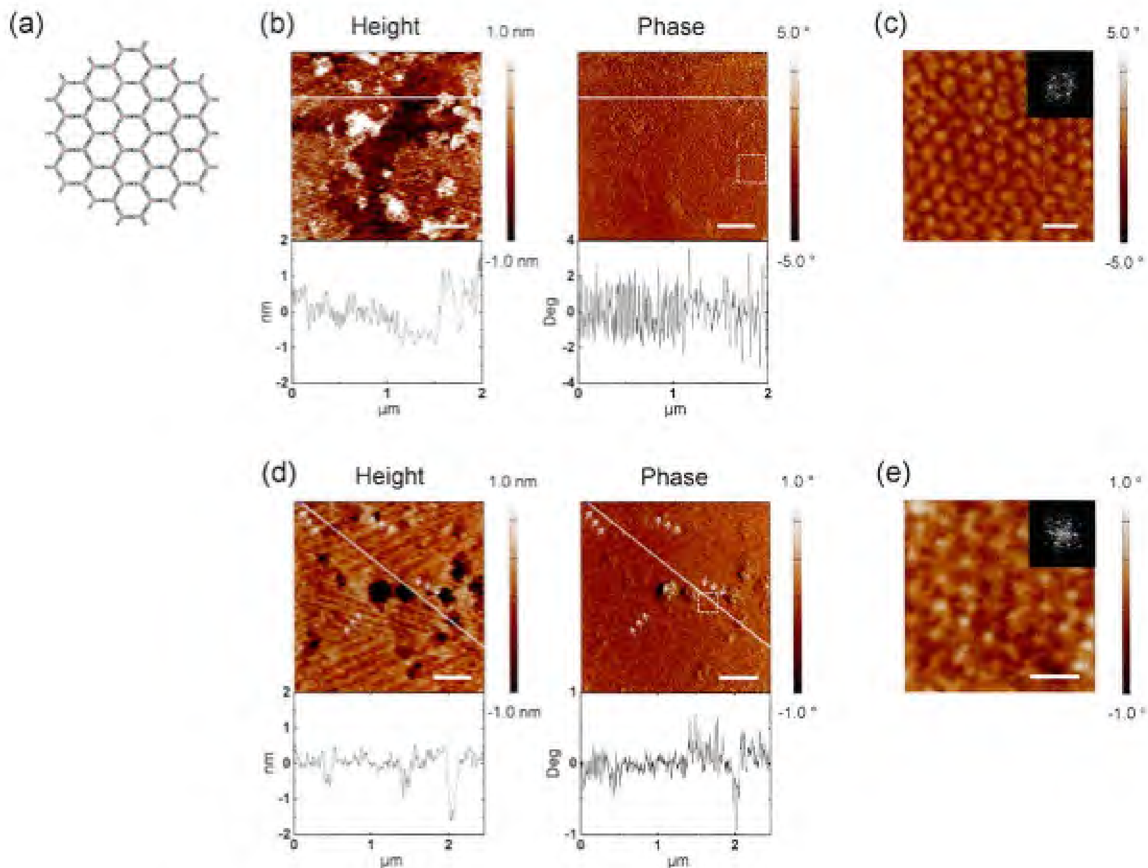

Figure 2.4. Fabrication of PMMA stamps by replication over hexagonal DNA 2D arrays. (a) Scheme of hexagonal DNA 2D arrays assembled from 3-point-star motifs. (b) AFM height (left) and phase (right) images of DNA 2D arrays assembled on the silicon wafer (top) and the corresponding cross-sections (bottom). (c) Zoom-in view of the area in the white dashed box in b. The inset is the Fourier transform pattern of the image in c. (d) AFM height (left) and phase (right) images of the PMMA stamps (top) and the corresponding cross-sections (bottom). (e) Zoom-in view of the area in the white dashed box in d. The inset is the Fourier transform pattern of the image in e. White arrows indicate the replicated patterns on PMMA. Scale bars in b and d represent 400 nm, and scale bars in c and e represent 50 nm.

To probe the resolution limit of this method, the feature size of the DNA nanostructures is further decreased to an individual DNA double helix. λ-DNA, a double-stranded phage DNA with a length of *ca.* 16 µm, was employed as a master template. The height and width (fwhm) of the individual λ-DNA were measured to be 0.3 ± 0.1 nm and 14.7 ± 3.2 nm, respectively (**Figures 2.5a**), although bundling of the λ-DNA was observed as well. After the replication, narrow 1D trenches with a depth of 0.4 ± 0.1 nm and a width (fwhm) of 11.1 ± 1.7 nm were observed on the PMMA stamp (**Figures 2.5b**), which represent the negative replica of the individual λ-DNA. This result suggests that even a single DNA double strand of a diameter of 2 nm might serve as a master template for the pattern transfer, suggesting the possibility of applying this method to pattern molecular-scale features.

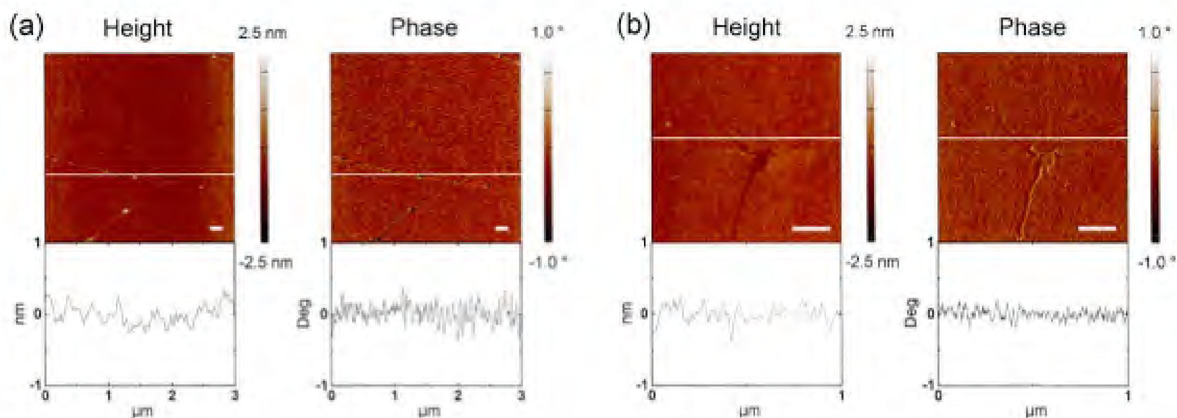

Figure 5. Fabrication of PMMA stamps by replication over the λ-DNA. AFM height (left) and phase (right) images of (a) λ-DNA deposited on the silicon wafer and (b) the replica of λ-DNA patterns on PMMA stamps. Corresponding cross-sections are shown at the bottom. Scale bars represent 200 nm.

All of the nanostructures tested above are either 1D linear structures or 2D nanostructures with periodic patterns. To increase the complexity of the patterns on the stamp, triangular DNA origami nanostructures[53, 71] were employed as master templates for the pattern transfer. The triangular DNA origami is composed of a single layer of DNA double strands with a theoretical height of 2 nm and contains three trapezoidal domains. The edges of the adjacent trapezoidal domains are connected by the bridging staple strands, forming three small triangular holes at each vertex and one large triangular hole in the center (**Figure 2.6a**). According to the design, the inner length (the length of the sides of the central triangular hole), outer length, and full width at half-maximum (fwhm) of the trapezoidal sides of the DNA triangles are 55.0 nm, 129.6 nm and 27.0 nm, respectively. AFM images show that the DNA triangles were randomly distributed on the silicon wafer and the central, large triangular holes were clearly visible (**Figures 2.6b**). Because of the resolution limitation of the AFM images, the bridging staple strands between the trapezoidal domains were not visible. As a result, the three smaller triangular holes at the vertex were shown as a linear gap. The tangling loop was visible in some DNA triangles; in other structures, the tangling loops might have attached on top of the DNA triangle or beneath the structure so that they were not visible. According to the AFM cross-section analysis, the height, inner length, outer length, and width (fwhm) of the trapezoidal sides of the DNA triangles were 1.6 ± 0.1 nm, 45.6 ± 2.0 nm, 131.2 ± 5.4 nm, and 38.0 ± 3.1 nm, respectively. The measured height of DNA nanostructures in AFM images might vary due to the differences in the probe-substrate and probe-sample interactions.[79] Due to the AFM probe convolution, the measured outer length and side width of DNA triangles increased compared with the theoretical value, and the measured inner length of DNA triangles was smaller than the theoretical value.

After the pattern transfer, triangular trenches appeared on the PMMA film, resembling the shape of the DNA origami (**Figures 2.6c**). Even the pattern of the tangling loop had been transferred to the PMMA stamp in some cases. The averaged depth, inner length, outer length, and width (fwhm) of the triangular trenches were 1.0 ± 0.2 nm, 54.3 ± 2.6 nm, 126.8 ± 3.8 nm, and 26.5 ± 3.1 nm, respectively. The decreased depth of the trenches is attributed to the removal of the salts during the pattern transfer. The inner length, outer length, and width of the triangular trenches are all consistent with the design. Similar to the DNA master templates, the small triangular holes did not show up on the PMMA stamps. Instead, we observed small bumps at the vertices of the triangular trenches, which is the replica of the gaps between the trapezoidal domains. As the feature size of the DNA master template decreases, especially when nanometer-sized holes exist in the DNA master template, PMMA might not be able to fully fill the holes during the pattern transfer, resulting in the decreased height and missing features in the PMMA replica. These results demonstrate that the overall features of the triangular DNA origami can be successfully transferred to the PMMA stamps with high fidelity, and the local features (*ca.* sub-5 nm) can be replicated to some extent.

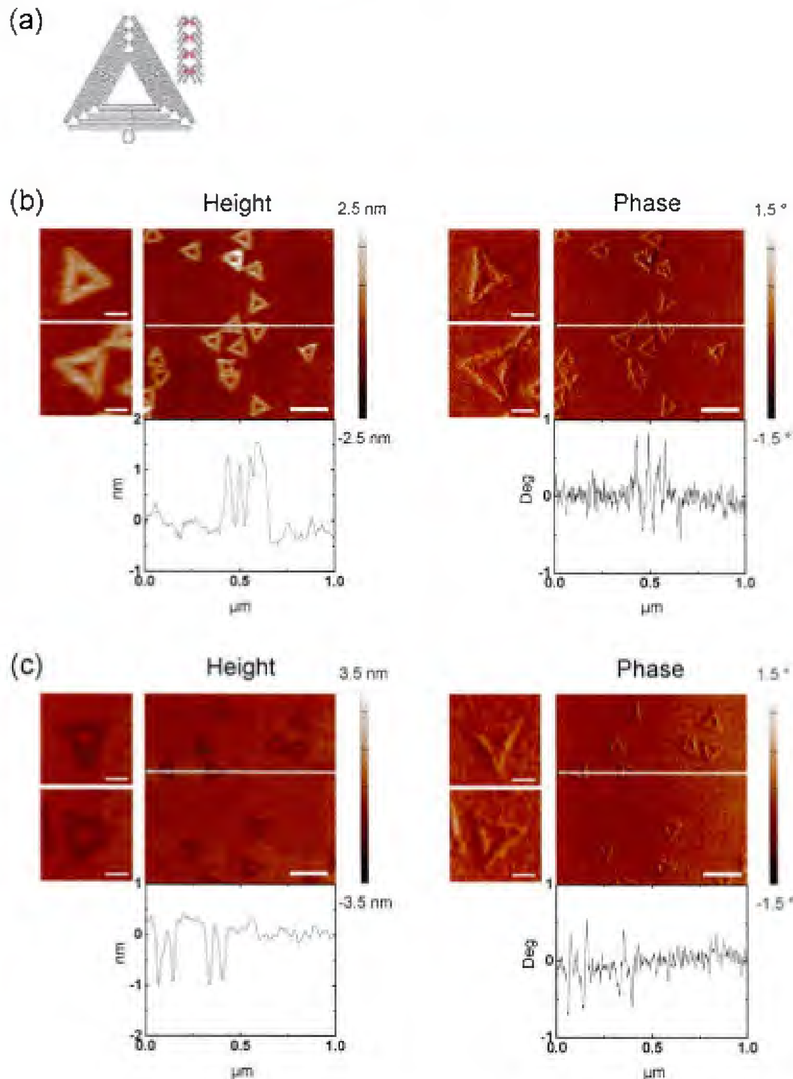

Figure 2.6. Fabrication of PMMA stamps by replication over the triangular DNA origami. (a) Folding path of the DNA scaffold strand in the DNA triangle. Red lines represent staple strands bridging the trapezoidal sides. Reprinted by permission from Macmillan Publishers Ltd: Nature (reference 30), copyright 2006. (b) AFM height (left) and phase (right) images of the DNA triangles deposited on a silicon wafer (top) and the corresponding cross-sections (bottom). (c) AFM height (left) and phase (right) images of triangular patterns on PMMA stamps (top) and the corresponding cross-sections (bottom). Zoomed-in images are on the left of the corresponding images. Scale bars represent 200 nm (zoomed-out images) or 50 nm (zoomed-in images).

Besides PMMA, other polymers such as PLLA could also be used as the stamp material in our method (**Figures 2.7**). Both DNA triangles and DNA nanotubes could be precisely replicated to the PLLA stamps. Similar to the pattern transfer from DNA triangles to the PMMA stamp, the tangling loops and the gaps between the trapezoidal domains could be also transferred to the PLLA stamp. AFM cross-sections indicate that the averaged depth and width (fwhm) of the triangular trenches on the PLLA stamps were 1.1 ± 0.2 nm and 27.1 ± 6.0 nm, respectively. The replication to the PLLA stamps offers a comparable resolution as observed for the PMMA stamps, demonstrating the potential for replicating DNA nanostructure patterns into a wider range of polymers.

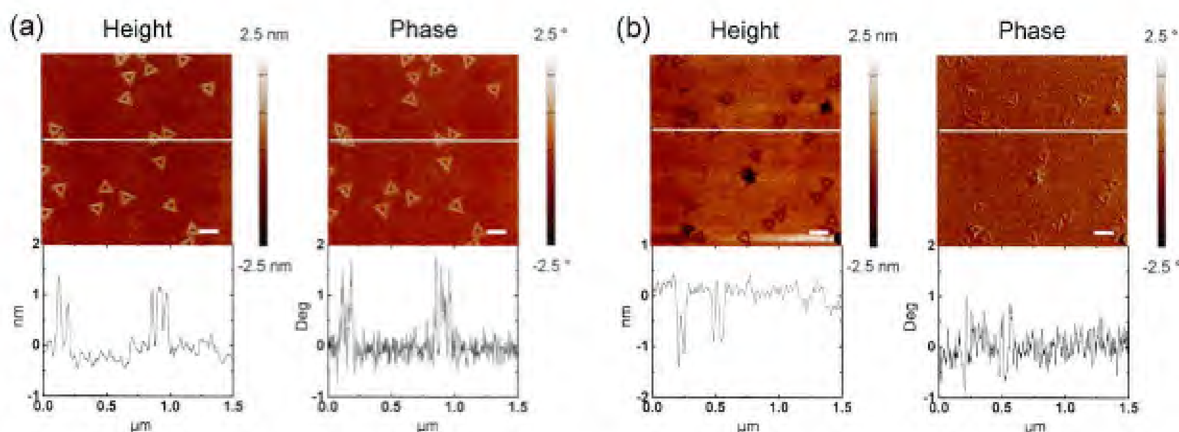

Figure 2.7. Fabrication of PLLA stamps by replication over the triangular DNA origami. (a) AFM height (left) and phase (right) images of DNA triangles deposited on a silicon wafer (top) and the corresponding cross-sections (bottom). (b) AFM height (left) and phase (right) images of triangular patterns on the PLLA stamps (top) and the corresponding cross-sections (bottom). Scale bars represent 150 nm.

To evaluate the yield of the replication process and its impact on the DNA master template, we imaged the DNA master templates and the polymer stamps in the same location (**Figures 2.8**). **Figures 2.8a** and **2.8d** show the topography and phase image of the DNA nanotubes on the silicon wafer, respectively. The corresponding negative replica on the polymer stamp (**Figures 2.8c** and **2.8f**) matched well with the DNA master templates (**Figures 2.8a** and **2.8d**), demonstrating a faithful pattern transfer. However, the nanotubes were partially damaged after the replication (**Figures 2.8b** and **2.8e**), which we attribute to the water used to separate the

master template and the stamp. To confirm the effect of water, we first used less water and decreased the incubation time (*i.e.*, the time between adding water to the silicon wafer and peeling off the polymer stamp). As a result, less DNA damage was observed. In addition, DNA nanotubes were also replicated to the a-PFPE polymer stamp, during which process water was not used. In addition, the AFM phase image also shows that the DNA nanostructure template was not trapped in the polymer stamps. Since the phase image is sensitive to the chemical composition, if DNA nanostructures were trapped in the trenches, the features would be visible in the phase image but not in the height image. Therefore, the yield of the pattern transfer can be assessed by examining the consistency between AFM height and phase images. In all the figures mentioned above, the position and shape of the features in the height and phase images matched with each other, suggesting the absence of trapped DNA nanostructures in the polymer stamps.

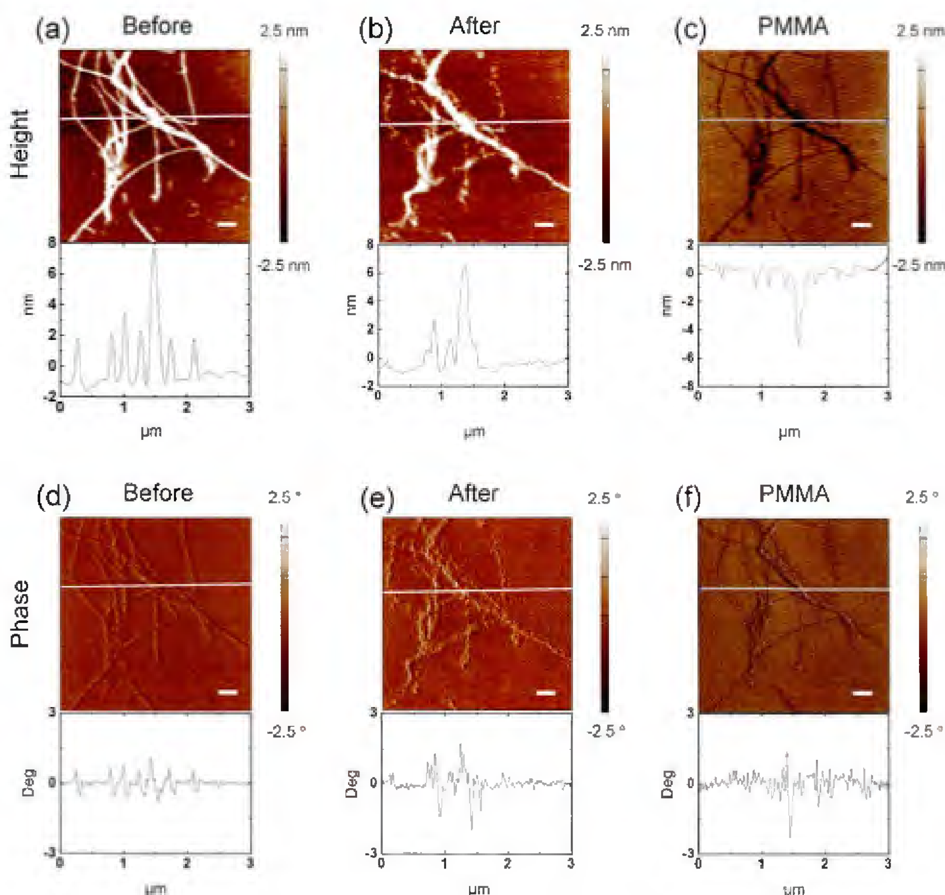

Figure 2.8. Comparison of features of the same location on the DNA master template and the polymer stamp. AFM height images and cross-sections of DNA nanotubes deposited on a silicon wafer (a) before and (b) after the replication to PMMA stamps, and (c) PMMA replica of the same area. (d) to (f) show the corresponding phase images and cross-sections. Scale bars represent 300 nm. Note: images (c) and (f) were flipped horizontally to match the orientation of the DNA master template.

In addition to the high yield of replication, the DNA master templates can be also used in a repeated manner to transfer the pattern to the a-PFPE stamp. **Figures 9** and **S13** show the AFM images of the DNA master templates before the replication process and after the 5th and 10th replication. The features of the DNA master templates were not damaged during the 10 times of replication. The repeated use of DNA master templates would greatly reduce the cost and facilitate its applications. We note that DNA master templates cannot be repeatedly used to transfer the pattern to PMMA or PLLA stamps at this stage because water, which is used to release the stamp, may damage the features of the DNA templates as mentioned above. To achieve the repeated use of the DNA master templates, polymers with low surface energy (*e.g.*, a-PFPE) should be employed to facilitate the separation of the stamp from the master template without the help of water. Alternatively, it is also possible to protect the DNA nanostructures using a nanometer-thin oxide coating (*e.g.*, Al_2O_3) grown by atomic layer deposition.[67]

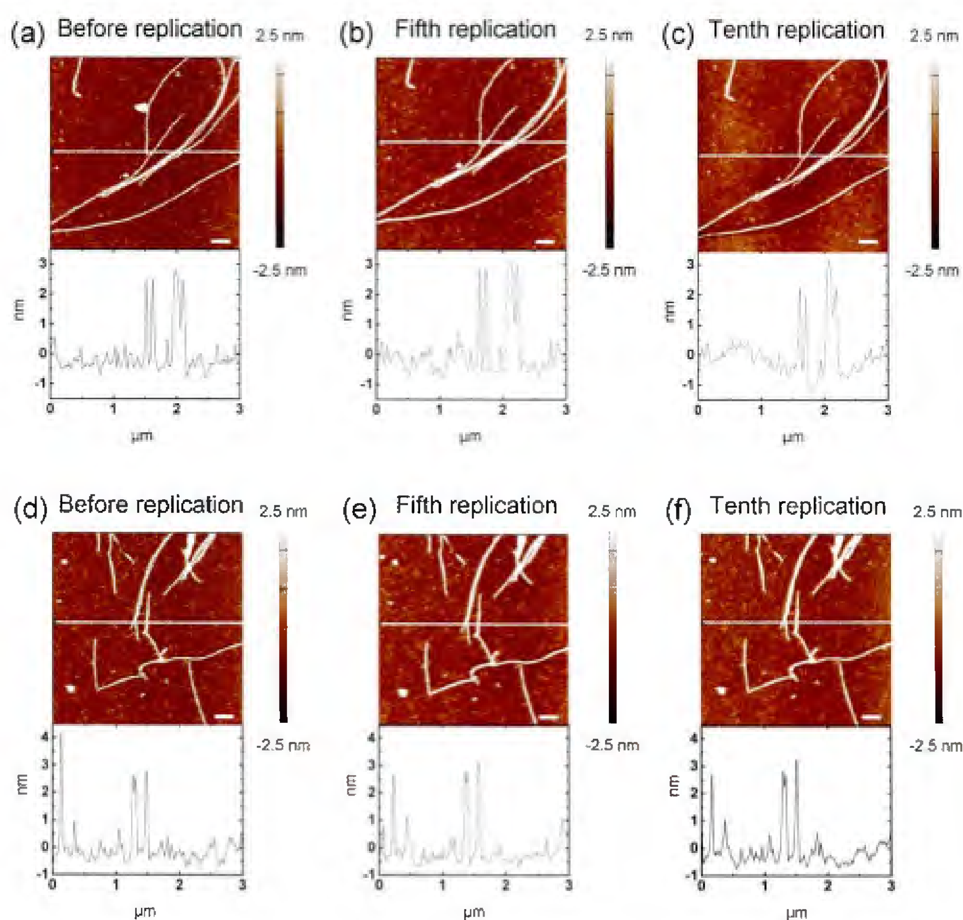

Figure 2.9. AFM height images of DNA nanotubes in two different locations (a, d) before the pattern transfer and after the (b, e) fifth and (c, f) tenth pattern transfer to the a-PFPE stamp (top). Corresponding cross-sections are shown at the bottom. Scale bars represent 300 nm.

The resulting polymer stamp could serve as a mold to transfer the pattern to other materials. **Figure 2.10** shows the replica molding of nanotube patterns on a PMMA stamp into a photo-curable a-PFPE.[80] In this experiment, the a-PFPE prepolymer was spin cast as a thin film on the PMMA stamps with the DNA nanotube relief and then cured under UV illumination. Due to the low surface energy of a-PFPE, the PMMA and a-PFPE films could be easily separated. A DNA nanotube pattern was observed on the a-PFPE film with a height of 2.5 ± 0.5 nm and a width of 41.6 ± 6.9 nm, demonstrating a faithful pattern transfer from PMMA stamps to the a-PFPE polymer film (**Figures 2.10**). Compared with the DNA nanotube master templates, both the depth/height and width of the patterns on the PMMA and a-PFPE were smaller. The average height/depth and width of DNA nanotube master templates, PMMA trenches, and nanotube patterns on the a-PFPE were 4.0 nm and 67.1 nm, 3.2 nm and 39.7 nm, and 2.5 nm and 41.6 nm, respectively. The exact reason for this decrease in dimensions is not clear at this stage. One possibility is that the removal of the salt residues during the fabrication of the PMMA stamp leads to the smaller size. We also note that a similar decrease in the feature size was previously reported on replicating a carbon nanotube pattern to the a-PFPE and then to the polyurethane.[80] In addition, the surface roughness of the a-PFPE film was measured to be 322.7 pm, which is much larger than that of the PMMA stamp (158.2 pm) but similar to that of the a-PFPE stamp (412.8 pm) that was produced from the DNA master templates. High surface roughness of a-PFPE mold was also reported before,[80] suggesting that it is likely an intrinsic property of this material and not a result from the molding process.

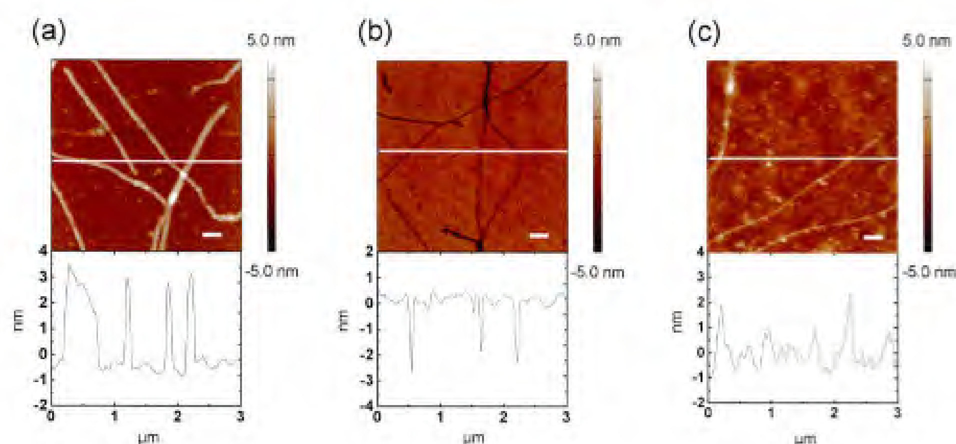

Figure 2.10. AFM height images of (a) DNA nanotubes on a silicon wafer, (b) DNA nanotube patterns on the PMMA stamp, and (c) DNA nanotube pattern on an a-PFPE substrate transferred from the PMMA stamp by the replica molding. Corresponding cross-sections are shown at the bottom. Scale bars represent 300 nm. Note: (a) and (b) are also shown in **Figure 2.2**.

Finally, we investigated the repeated use of the polymer stamps for the application of replica molding. We found that the polymer stamp film often delaminated from the PDMS backing layer and broke during the separation of the stamp from the mold. We attribute this observation to the micrometer-scale thinness of the stamp and its low affinity to PDMS. Part of the polymer stamp film remained on the PDMS backing layer and from which we were able to verify that the

nanoscale features there were not damaged after molding the a-PFPE film. Therefore, the polymer stamps should be reusable if an alternative molding process could be developed to protect the physical integrity of the polymer stamp. We note that others have reported the repeated use of polymer stamps, including PMMA, for replica molding and other nanoscale patterning applications.[81-88] Work is underway to fully explore the applications of the polymer stamps that we produced in this study.

CONCLUSIONS

We have demonstrated a general method of fabricating polymer stamps using DNA nanostructure master templates with high fidelity. DNA nanotubes, 1D λ-DNA, 2D DNA brick crystals with 3D features, hexagonal DNA 2D arrays, and triangular DNA origami have been tested as master templates to replicate their features to PMMA and PLLA. The resulting PMMA stamp has been applied as a mold to transfer the pattern to photo-crosslinked a-PFPE. In addition to replica molding, the polymer stamp can be potentially used in many other applications, in particular contact printing of small molecules and proteins.[27-28, 88-89] Since DNA master templates with diverse features can be rationally designed and constructed, our method could enable the fabrication of polymer stamps with varieties of nanoscale features, some of which (*e.g.*, alphabets) are inaccessible by other self-assembly methods. The integration of DNA nanotechnology with soft lithography offers alternative master templates and enriches the nanoscale features of polymer stamps to facilitate their applications.

To apply DNA nanostructures in the scalable nanofabrication, the limitation of large-area patterning in our method needs to be overcome. High-throughput nano-patterning is important for the nanofabrication and has been realized by e-beam lithography[32-33] and directed self-assembly of block copolymer.[38-40] However, the difficulties of controlling deposition of DNA nanostructures and defects in the self-assembled DNA nanostructures limit their applications in large-area patterning. Further studies are still needed to address these challenges. In addition, the technical issues associated with the repeated use of the polymer stamp in our method need to be overcome. At the current stage, this challenge could be compensated by generating multiple copies of the polymer stamps based on a DNA master template. Ways to increase the chemical and mechanical stability of the DNA master template (*e.g.*, by a conformal coating of an inorganic oxide film[66-67]) have been explored and published in peer reviewed journals.

References

1. Ho, J. C.; Yerushalmi, R.; Jacobson, Z. A.; Fan, Z.; Alley, R. L.; Javey, A., Controlled nanoscale doping of semiconductors via molecular monolayers. *Nat Mater* **2008,** *7* (1), 62-67.
2. Ho, J. C.; Yerushalmi, R.; Smith, G.; Majhi, P.; Bennett, J.; Halim, J.; Faifer, V. N.; Javey, A., Wafer-Scale, Sub-5 nm Junction Formation by Monolayer Doping and Conventional Spike Annealing. *Nano Lett* **2009,** *9* (2), 725-730.
3. Smith, R. K.; Lewis, P. A.; Weiss, P. S., Patterning self-assembled monolayers. *Prog. Surf. Sci.* **2004,** *75* (1-2), 1-68.

4. Wilbur, J. L.; Kumar, A.; Biebuyck, H. A.; Kim, E.; Whitesides, G. M., Microcontact printing of self-assembled monolayers: applications in microfabrication. *Nanotechnology* **1996,** *7* (4), 452-457.
5. Herzer, N.; Hoeppener, S.; Schubert, U. S., Fabrication of patterned silane based self-assembled monolayers by photolithography and surface reactions on silicon-oxide substrates. *Chem. Commun. (Cambridge, U. K.)* **2010,** *46* (31), 5634-5652.
6. Xia, Y.; Zhao, X.-M.; Whitesides, G. M., Pattern transfer: Self-assembled monolayers as ultrathin resists. *Microelectron. Eng.* **1996,** *32* (1-4), 255-268.
7. Schaal, P. A.; Besmehn, A.; Maynicke, E.; Noyong, M.; Beschoten, B.; Simon, U., Electrically Conducting Nanopatterns Formed by Chemical e-Beam Lithography via Gold Nanoparticle Seeds. *Langmuir* **2012,** *28* (5), 2448-2454.
8. Weimann, T.; Geyer, W.; Hinze, P.; Stadler, V.; Eck, W.; Golzhauser, A., Nanoscale patterning of self-assembled monolayers by e-beam lithography. *Microelectron. Eng.* **2001,** *57-58*, 903-907.
9. Battaglini, N.; Qin, Z.; Campiglio, P.; Repain, V.; Chacon, C.; Rousset, S.; Lang, P., Directed Growth of Mixed Self-Assembled Monolayers on a Nanostructured Template: a Step toward the Patterning of Functional Molecular Domains. *Langmuir* **2012,** *28* (42), 15095-15105.
10. Bulliard, X.; Benayad, A.; Ihn, S.-G.; Yun, S.; Park, J.-H.; Choi, W.; Choi, Y. S.; Kim, Y., Autocatalytic effect of amine-terminated precursors in mixed self-assembled monolayers. *RSC Adv.* **2013,** *3* (4), 1112-1118.
11. Stan, D.; Mihailescu, C.-M.; Iosub, R.; Moldovan, C.; Savin, M.; Baciu, I., Electrochemical studies of homogeneous self-assembled monolayers versus mixed self-assembled monolayers on gold electrode for label free detection of heart fatty acid binding protein. *Thin Solid Films* **2012,** *526*, 143-149.
12. Luessem, B.; Mueller-Meskamp, L.; Karthaeuser, S.; Waser, R.; Homberger, M.; Simon, U., STM Study of Mixed Alkanethiol/Biphenylthiol Self-Assembled Monolayers on Au(111). *Langmuir* **2006,** *22* (7), 3021-3027.
13. Cancino, J.; Machado, S. A. S., Microelectrode array in mixed alkanethiol self-assembled monolayers: Electrochemical studies. *Electrochim. Acta* **2012,** *72*, 108-113.
14. Unruh, D. A.; Mauldin, C.; Pastine, S. J.; Rolandi, M.; Frechet, J. M. J., Bifunctional Patterning of Mixed Monolayer Surfaces Using Scanning Probe Lithography for Multiplexed Directed Assembly. *J. Am. Chem. Soc.* **2010,** *132* (20), 6890-6891.
15. Yu, J.-J.; Tan, Y. H.; Li, X.; Kuo, P.-K.; Liu, G.-Y., A Nanoengineering Approach to Regulate the Lateral Heterogeneity of Self-Assembled Monolayers. *J. Am. Chem. Soc.* **2006,** *128* (35), 11574-11581.
16. Xu, S.; Liu, G.-y., Nanometer-Scale Fabrication by Simultaneous Nanoshaving and Molecular Self-Assembly. *Langmuir* **1997,** *13* (2), 127-129.
17. Gorman, C. B.; Carroll, R. L.; He, Y.; Tian, F.; Fuierer, R., Chemically Well-Defined Lithography Using Self-Assembled Monolayers and Scanning Tunneling Microscopy in Nonpolar Organothiol Solutions. *Langmuir* **2000,** *16* (15), 6312-6316.
18. Kumar, T. A.; Bardea, A.; Shai, Y.; Yoffe, A.; Naaman, R., Patterning Gradient Properties from Sub-Micrometers to Millimeters by Magnetolithography. *Nano Lett.* **2010,** *10* (6), 2262-2267.
19. Bardea, A.; Baram, A.; Tatikonda, A. K.; Naaman, R., Magnetolithographic Patterning of Inner Walls of a Tube: A New Dimension in Microfluidics and Sequential Microreactors. *J. Am. Chem. Soc.* **2009,** *131* (51), 18260-18262.

20. He, Y.; Ye, T.; Ribbe, A. E.; Mao, C. D., DNA-Templated Fabrication of Two-Dimensional Metallic Nanostructures by Thermal Evaporation Coating. *Journal of the American Chemical Society* **2011,** *133* (6), 1742-1744.
21. Deng, Z. X.; Mao, C. D., Molecular Lithography with DNA Nanostructures. *Angew. Chem. Int. Edit.* **2004,** *43* (31), 4068-4070.
22. Magonov, S. N.; Elings, V.; Whangbo, M. H., Phase imaging and stiffness in tapping-mode atomic force microscopy. *Surface Science* **1997,** *375* (2-3), L385-L391.
23. Martinez, N. F.; Garcia, R., Measuring phase shifts and energy dissipation with amplitude modulation atomic force microscopy. *Nanotechnology* **2006,** *17* (7), S167-S172.
24. Xia, Y. N.; Whitesides, G. M., Soft lithography. *Annu. Rev. Mater. Sci.* **1998,** *28*, 153-184.
25. Gates, B. D.; Xu, Q. B.; Stewart, M.; Ryan, D.; Willson, C. G.; Whitesides, G. M., New Approaches to Nanofabrication: Molding, Printing, and Other Techniques. *Chem. Rev.* **2005,** *105* (4), 1171-1196.
26. Rogers, J. A.; Nuzzo, R. G., Recent Progress in Soft Lithography. *Mater. Today* **2005,** *8* (2), 50-56.
27. Qin, D.; Xia, Y.; Whitesides, G. M., Soft Lithography for Micro- and Nanoscale Patterning. *Nat. Protoc.* **2010,** *5* (3), 491-502.
28. Lipomi, D. J.; Martinez, R. V.; Cademartiri, L.; Whitesides, G. M., Soft Lithographic Approaches to Nanofabrication. In *Polymer Science: A Comprehensive Reference*, Matyjaszewski, K.; Möller, M., Eds. Elsevier Science: Oxford, 2012; Vol. 7, pp 211-231.
29. Lipomi, D. J.; Martinez, R. V.; Whitesides, G. M., Use of Thin Sectioning (Nanoskiving) to Fabricate Nanostructures for Electronic and Optical Applications. *Angew. Chem. Int. Edit.* **2011,** *50* (37), 8566-8583.
30. Xia, Y. N.; Rogers, J. A.; Paul, K. E.; Whitesides, G. M., Unconventional Methods for Fabricating and Patterning Nanostructures. *Chem. Rev.* **1999,** *99* (7), 1823-1848.
31. Pease, R. F.; Chou, S. Y., Lithography and Other Patterning Techniques for Future Electronics. *P. IEEE* **2008,** *96* (2), 248-270.
32. Wieland, M. J.; de Boer, G.; ten Berge, G. F.; van Kervinck, M.; Jager, R.; Peijster, J. J. M.; Slot, E.; Steenbrink, S.; Teepen, T. F.; Kampherbeek, B. J., MAPPER: High throughput maskless lithography. *Proc. SPIE* **2010,** *7637*.
33. Lin, B. J., Future of Multiple-E-Beam Direct-Write Systems. *Proc. SPIE* **2012,** *8323*.
34. Shim, W.; Braunschweig, A. B.; Liao, X.; Chai, J.; Lim, J. K.; Zheng, G.; Mirkin, C. A., Hard-tip, soft-spring lithography. *Nature* **2011,** *469* (7331), 516-521.
35. Gong, J.; Lipomi, D. J.; Deng, J.; Nie, Z.; Chen, X.; Randall, N. X.; Nair, R.; Whitesides, G. M., Micro- and Nanopatterning of Inorganic and Polymeric Substrates by Indentation Lithography. *Nano Lett.* **2010,** *10* (7), 2702-2708.
36. Haynes, C. L.; Van Duyne, R. P., Nanosphere Lithography: A Versatile Nanofabrication Tool for Studies of Size-Dependent Nanoparticle Optics. *J. Phys. Chem. B* **2001,** *105* (24), 5599-5611.
37. Hawker, C. J.; Russell, T. P., Block Copolymer Lithography: Merging "Bottom-Up" with "Top-Down" Processes. *MRS Bull.* **2005,** *30* (12), 952-966.
38. Stoykovich, M. P.; Muller, M.; Kim, S. O.; Solak, H. H.; Edwards, E. W.; de Pablo, J. J.; Nealey, P. F., Directed assembly of block copolymer blends into nonregular device-oriented structures. *Science* **2005,** *308* (5727), 1442-1446.

39. Ruiz, R.; Kang, H. M.; Detcheverry, F. A.; Dobisz, E.; Kercher, D. S.; Albrecht, T. R.; de Pablo, J. J.; Nealey, P. F., Density multiplication and improved lithography by directed block copolymer assembly. *Science* **2008,** *321* (5891), 936-939.
40. Jeong, S. J.; Kim, J. Y.; Kim, B. H.; Moon, H. S.; Kim, S. O., Directed self-assembly of block copolymers for next generation nanolithography. *Mater. Today* **2013,** *16* (12), 468-476.
41. Elhadj, S.; Rioux, R. M.; Dickey, M. D.; DeYoreo, J. J.; Whitesides, G. M., Subnanometer Replica Molding of Molecular Steps on Ionic Crystals. *Nano Lett.* **2010,** *10* (10), 4140-4145.
42. Xu, Q. B.; Mayers, B. T.; Lahav, M.; Vezenov, D. V.; Whitesides, G. M., Approaching zero: Using fractured crystals in metrology for replica molding. *J. Am. Chem. Soc.* **2005,** *127* (3), 854-855.
43. Hua, F.; Sun, Y. G.; Gaur, A.; Meitl, M. A.; Bilhaut, L.; Rotkina, L.; Wang, J. F.; Geil, P.; Shim, M.; Rogers, J. A., Polymer imprint lithography with molecular-scale resolution. *Nano Lett.* **2004,** *4* (12), 2467-2471.
44. Seeman, N. C., Nanomaterials Based on DNA. In *Annual Review of Biochemistry, Vol 79*, Kornberg, R. D.; Raetz, C. R. H.; Rothman, J. E.; Thorner, J. W., Eds. Annual Reviews: Palo Alto, 2010; Vol. 79, pp 65-87.
45. Lin, C. X.; Liu, Y.; Rinker, S.; Yan, H., DNA Tile Based Self-Assembly: Building Complex Nanoarchitectures. *Chemphyschem* **2006,** *7* (8), 1641-1647.
46. Aldaye, F. A.; Palmer, A. L.; Sleiman, H. F., Assembling Materials with DNA as the Guide. *Science* **2008,** *321* (5897), 1795-1799.
47. Rothemund, P. W. K.; Ekani-Nkodo, A.; Papadakis, N.; Kumar, A.; Fygenson, D. K.; Winfree, E., Design and Characterization of Programmable DNA Nanotubes. *J. Am. Chem. Soc.* **2004,** *126* (50), 16344-16352.
48. Liu, H. P.; Chen, Y.; He, Y.; Ribbe, A. E.; Mao, C. D., Approaching the limit: Can one DNA oligonucleotide assemble into large nanostructures? *Angew. Chem. Int. Edit.* **2006,** *45* (12), 1942-1945.
49. Yin, P.; Hariadi, R. F.; Sahu, S.; Choi, H. M. T.; Park, S. H.; LaBean, T. H.; Reif, J. H., Programming DNA Tube Circumferences. *Science* **2008,** *321* (5890), 824-826.
50. Tian, C.; Zhang, C.; Li, X.; Hao, C.; Ye, S.; Mao, C., Approaching the Limit: Can One DNA Strand Assemble into Defined Nanostructures? *Langmuir* **2014,** *30* (20), 5859-5862.
51. Ding, B. Q.; Sha, R. J.; Seeman, N. C., Pseudohexagonal 2D DNA Crystals from Double Crossover Cohesion. *J. Am. Chem. Soc.* **2004,** *126* (33), 10230-10231.
52. He, Y.; Chen, Y.; Liu, H. P.; Ribbe, A. E.; Mao, C. D., Self-Assembly of Hexagonal DNA Two-Dimensional (2D) Arrays. *J. Am. Chem. Soc.* **2005,** *127* (35), 12202-12203.
53. Rothemund, P. W. K., Folding DNA to create nanoscale shapes and patterns. *Nature* **2006,** *440* (7082), 297-302.
54. Wei, B.; Dai, M. J.; Yin, P., Complex Shapes Self-Assembled from Single-Stranded DNA Tiles. *Nature* **2012,** *485* (7400), 623-626.
55. Zhang, F.; Jiang, S. X.; Wu, S. Y.; Li, Y. L.; Mao, C. D.; Liu, Y.; Yan, H., Complex wireframe DNA origami nanostructures with multi-arm junction vertices. *Nat. Nanotechnol.* **2015,** *10* (9), 779-784.
56. Wang, P.; Wu, S.; Tian, C.; Yu, G.; Jiang, W.; Wang, G.; Mao, C., Retrosynthetic Analysis-Guided Breaking Tile Symmetry for the Assembly of Complex DNA Nanostructures. *J. Am. Chem. Soc.* **2016,** *138* (41), 13579-13585.

57. Han, D. R.; Pal, S.; Nangreave, J.; Deng, Z. T.; Liu, Y.; Yan, H., DNA Origami with Complex Curvatures in Three-Dimensional Space. *Science* **2011,** *332* (6027), 342-346.
58. Ke, Y. G.; Ong, L. L.; Shih, W. M.; Yin, P., Three-Dimensional Structures Self-Assembled from DNA Bricks. *Science* **2012,** *338* (6111), 1177-1183.
59. Li, X.; Zhang, C.; Hao, C. H.; Tian, C.; Wang, G. S.; Mao, C. D., DNA Polyhedra with T-Linkage. *ACS Nano* **2012,** *6* (6), 5138-5142.
60. Tian, C.; Li, X.; Liu, Z. Y.; Jiang, W.; Wang, G. S.; Mao, C. D., Directed Self-Assembly of DNA Tiles into Complex Nanocages. *Angew. Chem. Int. Edit.* **2014,** *53* (31), 8041-8044.
61. Liu, Z.; Tian, C.; Yu, J.; Li, Y.; Jiang, W.; Mao, C., Self-Assembly of Responsive Multilayered DNA Nanocages. *J. Am. Chem. Soc.* **2015,** *137* (5), 1730-1733.
62. Li, Y.; Tian, C.; Liu, Z.; Jiang, W.; Mao, C., Structural Transformation: Assembly of an Otherwise Inaccessible DNA Nanocage. *Angew. Chem. Int. Edit.* **2015,** *54* (20), 5990-5993.
63. Zhang, G.; Surwade, S. P.; Zhou, F.; Liu, H., DNA Nanostructure Meets Nanofabrication. *Chem. Soc. Rev.* **2013,** *42* (7), 2488-2496.
64. Jin, Z.; Sun, W.; Ke, Y.; Shih, C. J.; Paulus, G. L. C.; Wang, Q. H.; Mu, B.; Yin, P.; Strano, M. S., Metallized DNA Nanolithography for Encoding and Transferring Spatial Information for Graphene Patterning. *Nat. Commun.* **2013,** *4*, 1663.
65. Surwade, S. P.; Zhao, S. C.; Liu, H. T., Molecular Lithography Through DNA-Mediated Etching and Masking of SiO2. *J. Am. Chem. Soc.* **2011,** *133* (31), 11868-11871.
66. Surwade, S. P.; Zhou, F.; Wei, B.; Sun, W.; Powell, A.; O'Donnell, C.; Yin, P.; Liu, H. T., Nanoscale Growth and Patterning of Inorganic Oxides Using DNA Nanostructure Templates. *J. Am. Chem. Soc.* **2013,** *135* (18), 6778-6781.
67. Zhou, F.; Sun, W.; Ricardo, K. B.; Wang, D.; Shen, J.; Yin, P.; Liu, H., Programmably Shaped Carbon Nanostructure from Shape-Conserving Carbonization of DNA. *ACS Nano* **2016,** *10* (3), 3069-77.
68. Sun, W.; Boulais, E.; Hakobyan, Y.; Wang, W. L.; Guan, A.; Bathe, M.; Yin, P., Casting Inorganic Structures with DNA Molds. *Science* **2014,** *346* (6210), 1258361.
69. Pinheiro, A. V.; Han, D. R.; Shih, W. M.; Yan, H., Challenges and opportunities for structural DNA nanotechnology. *Nat. Nanotechnol.* **2011,** *6* (12), 763-772.
70. Kershner, R. J.; Bozano, L. D.; Micheel, C. M.; Hung, A. M.; Fornof, A. R.; Cha, J. N.; Rettner, C. T.; Bersani, M.; Frommer, J.; Rothemund, P. W. K.; Wallraff, G. M., Placement and Orientation of Individual DNA Shapes on Lithographically Patterned Surfaces. *Nat. Nanotechnol.* **2009,** *4* (9), 557-561.
71. Hung, A. M.; Micheel, C. M.; Bozano, L. D.; Osterbur, L. W.; Wallraff, G. M.; Cha, J. N., Large-Area Spatially Ordered Arrays of Gold Nanoparticles Directed by Lithographically Confined DNA Origami. *Nat. Nanotechnol.* **2010,** *5* (2), 121-126.
72. Gopinath, A.; Rothemund, P. W. K., Optimized Assembly and Covalent Coupling of Single-Molecule DNA Origami Nanoarrays. *ACS Nano* **2014,** *8* (12), 12030-12040.
73. Gopinath, A.; Miyazono, E.; Faraon, A.; Rothemund, P. W. K., Engineering and mapping nanocavity emission via precision placement of DNA origami. *Nature* **2016,** *535* (7612), 401-405.
74. Qu, J. H.; Hou, X. L.; Fan, W. C.; Xi, G. H.; Diao, H. Y.; Liu, X. D., Scalable Lithography from Natural DNA Patterns via Polyacrylamide Gel. *Sci. Rep.* **2015,** *5*.
75. Li, H.; Wu, J.; Huang, X.; Yin, Z.; Liu, J.; Zhang, H., A Universal, Rapid Method for Clean Transfer of Nanostructures onto Various Substrates. *ACS Nano* **2014,** *8* (7), 6563-6570.

76. Ke, Y.; Ong, L. L.; Sun, W.; Song, J.; Dong, M.; Shih, W. M.; Yin, P., DNA Brick Crystals with Prescribed Depths. *Nat. Chem.* **2014,** *6* (11), 994-1002.
77. Lee, J.; Kim, S.; Kim, J.; Lee, C. W.; Roh, Y.; Park, S. H., Coverage Control of DNA Crystals Grown by Silica Assistance. *Angew. Chem. Int. Edit.* **2011,** *50* (39), 9145-9149.
78. Sun, X. P.; Ko, S. H.; Zhang, C. A.; Ribbe, A. E.; Mao, C. D., Surface-Mediated DNA Self-Assembly. *J. Am. Chem. Soc.* **2009,** *131* (37), 13248-13249.
79. Kim, H.; Surwade, S. P.; Powell, A.; O'Donnell, C.; Liu, H., Stability of DNA Origami Nanostructure Under Diverse Chemical Environments. *Chem. Mater.* **2014,** *26* (18), 5265-5273.
80. Truong, T. T.; Lin, R.; Jeon, S.; Lee, H. H.; Maria, J.; Gaur, A.; Hua, F.; Meinel, I.; Rogers, J. A., Soft lithography using acryloxy perfluoropolyether composite stamps. *Langmuir* **2007,** *23* (5), 2898-2905.
81. Li, H. F.; Lin, J. M.; Su, R. G.; Cai, Z. W.; Uchiyama, K., A polymeric master replication technology for mass fabrication of poly(dimethylsiloxane) microfluidic devices. *Electrophoresis* **2005,** *26* (9), 1825-1833.
82. Martínez, E.; Pla-Roca, M.; Samitier, J., Micro/Nanopatterning of Proteins Using a Nanoimprint-Based Contact Printing Technique. In *Nanotechnology in Regenerative Medicine: Methods and Protocols*, Navarro, M.; Planell, J. A., Eds. Humana Press: Totowa, NJ, 2012; pp 79-87.
83. Gates, B. D.; Whitesides, G. M., Replication of vertical features smaller than 2 nm by soft lithography. *J. Am. Chem. Soc.* **2003,** *125* (49), 14986-14987.
84. Muhlberger, M.; Rohn, M.; Danzberger, J.; Sonntag, E.; Rank, A.; Schumm, L.; Kirchner, R.; Forsich, C.; Gorb, S.; Einwogerer, B.; Trappl, E.; Heim, D.; Schift, H.; Bergmair, I., UV-NIL fabricated bio-inspired inlays for injection molding to influence the friction behavior of ceramic surfaces. *Microelectron. Eng.* **2015,** *141*, 140-144.
85. Xia, Y. N.; McClelland, J. J.; Gupta, R.; Qin, D.; Zhao, X. M.; Sohn, L. L.; Celotta, R. J.; Whitesides, G. M., Replica molding using polymeric materials: A practical step toward nanomanufacturing. *Adv. Mater.* **1997,** *9* (2), 147-149.
86. Zhang, Y.; Lo, C. W.; Taylor, J. A.; Yang, S., Replica molding of high-aspect-ratio polymeric nanopillar arrays with high fidelity. *Langmuir* **2006,** *22* (20), 8595-8601.
87. Gilles, S.; Meier, M.; Prompers, M.; van der Hart, A.; Kugeler, C.; Offenhausser, A.; Mayer, D., UV nanoimprint lithography with rigid polymer molds. *Microelectron. Eng.* **2009,** *86* (4-6), 661-664.
88. Pla-Roca, M.; Fernandez, J. G.; Mills, C. A.; Martinez, E.; Samitier, J., Micro/nanopatterning of proteins via contact printing using high aspect ratio PMMA stamps and NanoImprint apparatus. *Langmuir* **2007,** *23* (16), 8614-8618.
89. Li, H. W.; Muir, B. V. O.; Fichet, G.; Huck, W. T. S., Nanocontact printing: A route to sub-50-nm-scale chemical and biological patterning. *Langmuir* **2003,** *19* (6), 1963-1965.